JOURNAL OF CHEMICAL INFORMATION AND MODELING

Article

pubs.acs.org/jcim

Idealized Models of Protofilaments of Human Islet Amyloid Polypeptide

Yiyu Li,[†] Ma'mon M. Hatmal,[‡] Ralf Langen,[‡,§] and Ian S. Haworth*[,†,‡]

[†]Department of Pharmacology and Pharmaceutical Sciences, University of Southern California, Los Angeles, California 90089, United States

[‡]Department of Biochemistry, University of Southern California, Los Angeles, California 90033-9151, United States

[§]Zilkha Neurogenetic Institute, University of Southern California, 1501 San Pablo Street, Los Angeles, California 90033, United States

Supporting Information

ABSTRACT: Fibrils formed by assembly of human islet amyloid polypeptide (hIAPP) are found in most patients with type II diabetes. Structurally, these fibrils are composed of multiple protofilaments and are characterized by extended beta sheets, variable helical twists, and different morphologies. We have previously derived models for the hIAPP protofilament using simulations constrained by data from EPR spectroscopy. In the current work, these models were used as a basis for generating idealized hIAPP protofilaments with symmetrical geometrical properties using a new algorithm, MFIBRIL. We show good agreement of the idealized protofilaments with experimental data for amino acid side chain orientations and geometrical features including the inter-β sheet distance and the protofilament radius. These idealized protofilaments can be used in MFIBRIL to generate fibril models that may be experimentally testable at the molecular level. MFIBRIL can also be used for building structures of any repetitive molecular assembly starting with a single building block obtained from any source.

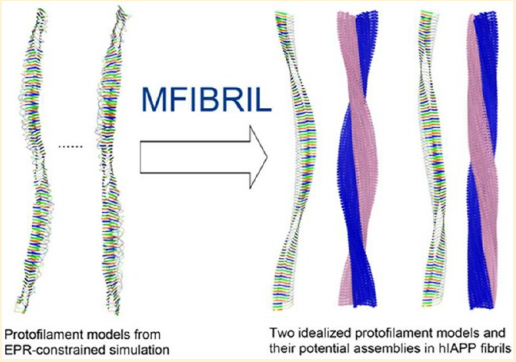

INTRODUCTION

Amyloidogenic peptides and proteins have the intrinsic ability to aggregate and form insoluble fibrils. These aggregates are associated with more than 40 human diseases, including Alzheimer's disease, Parkinson's disease, and prion diseases.[1] Human islet amyloid polypeptide (hIAPP) is a 37-residue peptide hormone cosecreted with insulin by pancreatic beta cells in response to an elevated glucose level. Among several physiological roles, soluble hIAPP facilitates the effects of insulin by stimulating neurons to reduce food intake.[2] However, misfolding and aggregation of hIAPP is toxic to beta cells[3−5] and hIAPP fibrils are found in >90% of patients with type II diabetes.[6] Understanding the structure of these fibrils and earlier aggregates on the fibril pathway may reveal the mechanism of hIAPP aggregation and facilitate the design of therapeutic agents and biomarkers for type II diabetes.

The structure of the hIAPP fibril is difficult to study directly, but structural information has been obtained by indirect methods. Fourier transform infrared spectroscopy and circular dichroism have shown that the fibril has a significant β-stranded component.[7,8] X-ray and electron diffraction data indicate that the β-strands are perpendicular to the fibril axis (i.e., a cross-β-structure) and that the spacing between successive β-strands is about 4.7 Å. A diffuse 9.5-Å reflection is also observed in X-ray diffraction data and is thought to be due to spacing between β-sheets.[9] Election paramagnetic resonance (EPR) spectroscopy shows that the β-strands are parallel and in-register; i.e., the same residues in neighboring peptides stack on each other.[1,6]

Electron microscopy (EM) has shown that hIAPP fibrils are polymorphous, with two major morphologies: a ribbonlike form and a left-handed twisted form.[10] The diameter of the fibrils typically varies from 80 to 150 Å[9,10] and the pitch of the twisted fibrils varies from about 250 to 500 Å.[9−11] Conventional and scanning transmission EM show that a hIAPP fibril consists of 2−4 or more protofilaments,[10] where a protofilament is defined as a single peptide stack. EM observations of fibril preparations have also shown some thinner structures of about 50 Å in diameter.[9,10]

We recently derived a family of models for protofilaments in twisted hIAPP fibrils using EPR spectroscopy and computational simulated annealing.[12] A key element in obtaining these models was computational refinement based on interspin label distances obtained using the double electron−electron resonance (DEER) method. The resulting family of protofilament models is characterized by stacked hIAPP monomers that form opposing ß-sheets and exhibit a left-handed helical twist. The two ß-strands of each monomer adopt out-of-plane positions and are staggered by about three peptide layers.[12]

Received: June 28, 2012

   dx.doi.org/10.1021/ci300300e | J. Chem. Inf. Model. XXXX, XXX, XXX−XXX

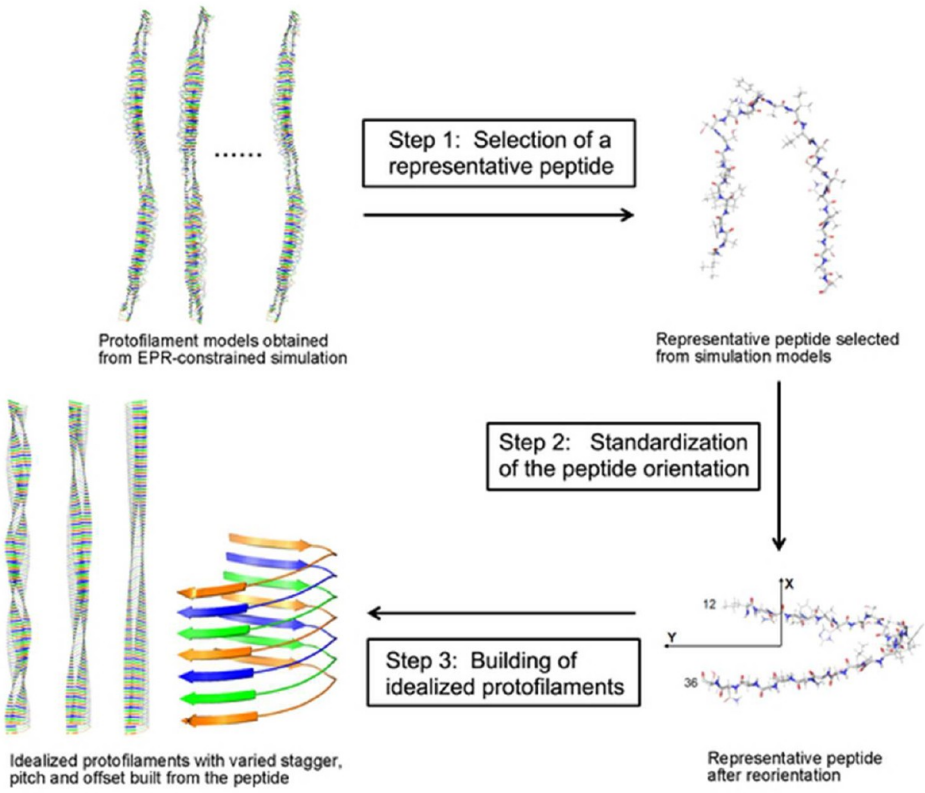

Figure 1. Flowchart showing the three steps in the MFIBRIL program.

The EPR-derived models provide many insights into the structure of the hIAPP protofilament. Our goal is to use these models as a basis for construction of potential hIAPP fibril models that may be validated with further EPR experiments. However, the resolution of the protofilament models is limited, particularly in regions that are less well constrained by experimental data. This leads to variability in the conformation of the constituent peptides and in the local helicity, which restricts our ability to understand the details of the protofilament and to build fibril models. Therefore, we developed an algorithm, MFIBRIL, to extract representative peptides from the models and use these peptides to generate idealized protofilaments with defined geometries. Here, we describe MFIBRIL and discuss its potential for generation of experimentally testable fibril models built from symmetrical and geometrically defined protofilaments.

METHODS

MFIBRIL. In describing the MFIBRIL algorithm, we refer to models of hIAPP protofilaments obtained from simulated annealing based on EPR constraints.[12] These calculations were performed on protofilaments comprising 101 peptides, with every fourth peptide carrying spin labels. Separate calculations were performed with constraints to produce protofilament models with different helical pitches and each calculation gave a family of ten protofilament models that were consistent with the EPR constraints.[12] In all families, the peptide unit adopted a horseshoe conformation, but with one ß-strand displaced with respect to the plane of the second ß-strand.[12]

Peptides with this general out-of-plane horseshoe conformation were used in MFIBRIL to build an idealized protofilament in three steps, as illustrated in Figure 1: (1) selection of a representative monomeric unit (peptide) from peptide aggregates, for example, a family of protofilament models obtained from simulated annealing; (2) standardization of the orientation of this peptide; (3) rebuilding of an idealized protofilament with a defined pitch, stagger, and axis offset (defined below) using multiple copies of the peptide. Using these three steps, we constructed idealized protofilaments starting with multiple peptides from each of the families of protofilament models. Each step is described in detail in the following sections.

We note that step 1 in this procedure is specifically focused on determination of a representative peptide from a family of protofilament models obtained from simulated annealing calculations for hIAPP. However, MFIBRIL can select representative peptides from any aggregate consisting of identical peptides with similar conformations. Step 1 can also be omitted and MFIBRIL can be used to build a repeating molecular assembly starting from a single unit from any source. The program is not restricted to models obtained from simulation or to molecular assemblies comprising only amyloidogenic peptides. MFIBRIL is available for use at http://chemsoft.hsc.usc.edu:8080/MFIBRIL/.

Step 1: Selection of Representative Peptides. Representative peptides are selected from a simulation data set of protofilament models[12] based on two criteria: the position of the Cα of each amino acid and the side chain direction. Each data set contains 10 models and each model includes 101 peptides.[12] First, all the peptides of a data set are aligned in PyMol[13] based on a user-defined region, for which we used residues 13−18 and 31−35 (the beta-strand regions) of peptide no. 50 in the sixth 101-peptide hIAPP protofilament model. Then, for each residue, a boundary cube is defined that covers all the Cα atoms from the same residue of different peptides.

dx.doi.org/10.1021/ci300300e | J. Chem. Inf. Model. XXXX, XXX, XXX−XXX

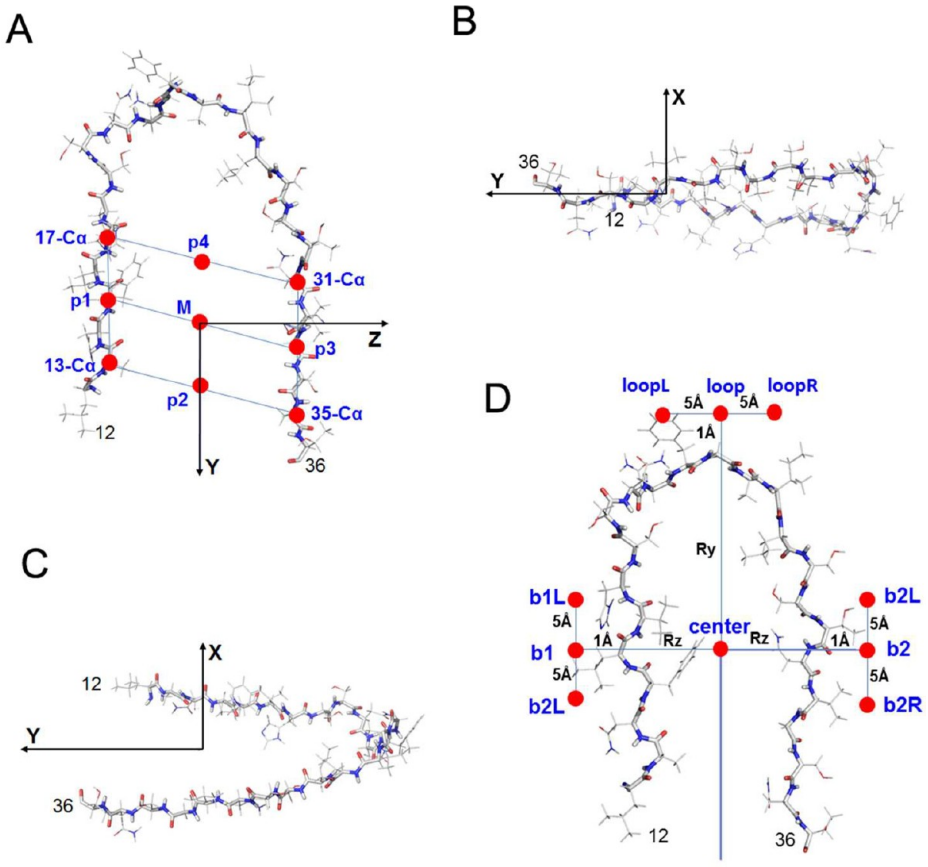

Figure 2. Definitions in the MFIBRIL program. (A) Orientation of the peptide in the *yz* plane at $x = 0$ and perpendicular to the fibril (*x*-)axis. (B) A different view of the oriented peptide, with the open end of the hairpin in the positive *y* direction. (C) Introduction of stagger into the peptide. (D) Different offsets of rotational axes (red dots). The ″center″ point is the default.

This cube is divided into 64 smaller subcubes of equal volume. The score of each subcube is given by the number of Cα atoms it contains. The "Cα score" of each residue in a particular peptide is equal to the score of the subcube in which the Cα atom resides, and the total Cα score of the peptide is the sum of the scores of all the residues in that peptide.

Step 2: Standardization of the Orientation of the Representative Peptides. The orientation of each representative peptide is standardized before building a protofilament. To standardize the orientation, a peptide plane is defined perpendicular to the fibril axis. In the hIAPP peptide, this plane is defined by three points (Figure 2A): P1, the midpoint of the Cα atoms of residues 13 and 17, P2, the midpoint of the Cα atoms of residues 13 and 35, and P3, the midpoint of the Cα atoms of residues 31 and 35. The peptide plane is then rotated to $x = 0$, and the peptide is shifted to point M, the midpoint of P2 and P4, where P4 is the midpoint of the Cα atoms of residues 17 and 31. Alternatively, users can choose the midpoint of P1 and P3 for point M. Finally, the peptide is rotated to project the line M−P2 as the *y*-axis in the $x = 0$ plane. This standardization procedure gives a hIAPP peptide with two β-strands that are almost in the same plane perpendicular to the *x*-axis, with the open end of the peptide in the positive *y* direction (Figure 2B). In this configuration, the *x*-axis is parallel to the growth axis of the protofilament.

Step 3: Building an Idealized Protofilament. hIAPP protofilaments are left-handed helices that contain peptides staggered by about three peptide layers.[12] To reproduce these geometrical properties, peptide stagger and helical pitch (Figure 2C) must be included in the idealized protofilaments. Furthermore, the helical axis of the protofilament may not be positioned centrally. Thus, MFIBRIL permits this axis to be offset to any (*x*,*y*) coordinate (Figure 2D).

The stagger of a peptide is defined by the offset of the two β-stands along the *x*-axis (Figure 2C) and specifically by the difference (in ångstrom) between the *x* coordinates of the Cα atoms of residues 13 and 35. For convenience, we refer to the stagger in terms of peptide spacing, where 1 "peptide spacing" is the distance between neighboring peptides and is 4.7 Å for hIAPP. To obtain a given stagger, the peptide is rotated around the *y*-axis to give the appropriate difference between the *x* coordinates of Cα(13) and Cα(35), without changing the peptide conformation.

The pitch of the protofilament is defined with the assumption that each peptide rotates by the same angle to achieve the final pitch. That is, given a pitch = *p* Å, every peptide performs a clockwise rotation with angle $\alpha = 360°/(p/\text{spacing})$. To achieve a left-handed pitch, *p* must be positive. The axis for helical rotation is parallel to the *x*-axis (Figure 2C).

The offset is defined as the cross point of the rotational axis and the plane $x = 0$ and can be defined by the user. A built-in reference point is the ″center″ (Figure 2D) of the peptide at point C $(0, y_0, z_0)$, where y_0 is the midpoint between the two Cα atoms that have the largest and smallest *y* coordinates (y_1 and y_2), and z_0 is the midpoint of the Cα atoms that have the largest and smallest *z* coordinates (z_1 and z_2). The offset of the rotational axis is defined from the reference point. Other reference points (identified as red dots with blue text in Figure

dx.doi.org/10.1021/ci300300e | J. Chem. Inf. Model. XXXX, XXX, XXX−XXX

Table 1. Geometrical Analysis of hIAPP Protofilament Models Built in MFIBRIL

MFIBRIL model no.	stagger (peptides)	pitch (Å)	offset[a]	4_ nc	4_ 250	4_ 500	4_ 1000	total[b]	sheet−sheet (Å)	radius (Å)
1	3	250	center	18	19	24	19	80	8.3 ± 1.6	17.5 ± 0.9
2	3	500	center	18	19	24	19	80	10.6 ± 1.6	17.5 ± 0.9
3	3	1000	center	18	19	24	19	80	11.7 ± 1.7	17.5 ± 0.9
4	3	2000	center	18	19	24	19	80	12.3 ± 1.7	17.5 ± 0.9
5	2	500	center	23	23	25	24	95	14.9 ± 1.3	18.2 ± 0.8
6	4	500	center	16	13	11	3	43	5.2 ± 1.6	16.6 ± 0.9
7	3	250	loop	16	16	11	1	44	3.8 ± 0.9	33.0 ± 1.7
8	3	500	loop	18	19	24	18	79	7.8 ± 1.6	33.6 ± 1.7
9	3	1000	loop	18	19	24	19	80	10.3 ± 1.6	33.6 ± 1.7
10	3	250	b1	18	19	24	18	79	10.0 ± 1.4	23.8 ± 1.2
11	3	500	b1	18	19	24	19	80	11.2 ± 1.6	23.8 ± 1.2
12	3	1000	b1	18	19	24	19	80	12.0 ± 1.6	23.8 ± 1.2
13	3	250	b2	18	19	24	19	80	7.9 ± 1.8	22.9 ± 1.2
14	3	500	b2	18	19	24	19	80	10.3 ± 1.7	22.9 ± 1.2
15	3	1000	b2	18	19	24	19	80	11.6 ± 1.7	22.9 ± 1.2

[a]For definitions, see Figure 2D. [b]The sum of the previous four columns. Each of these columns indicates the sample size of each data set (i.e., the number of protofilaments modeled from different representative peptides obtained from each data set).

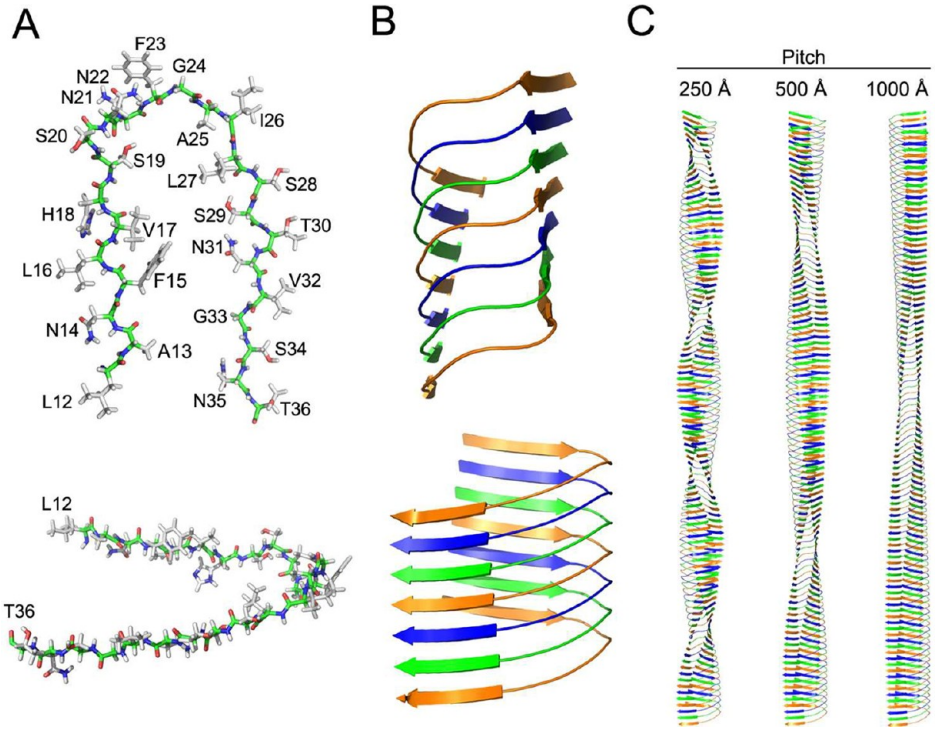

Figure 3. (A) Two views of a consensus IAPP peptide (residues 12−36) obtained from MFIBRIL analysis of simulation models. (B) Stacking of the same peptide in a protofilament built in MFIBRIL. The stagger of three peptides is illustrated by the coloring of orange, blue, and green. It is apparent that one β-strand of, for example, an orange peptide is in the same plane as the other beta strand of the next orange peptide in the structure. (C) Protofilament models (101 peptides) built from the consensus peptide by MFIBRIL, with staggers of three peptides and pitches of 250, 500, and 1000 Å. These are model nos. 1, 2, and 3, respectively, in Table 1.

2D, where $R_y = y_1 - y_0$ and $R_z = z_1 - z_0$) can be defined to build potential fibril models based on peptide−peptide interactions via the loop or β-strands.

Geometrical Analysis of Idealized Protofilaments. Analysis of the geometric properties of idealized protofilaments can also be performed using MFIBRIL. The sheet−sheet distance (the distance between the two β-sheets in the protofilament) and radius were determined for idealized protofilaments with variation of peptide stagger, helical pitch, and axis offset. These data were compared with those obtained in EPR-constrained simulation models[12] and through direct experiments.[9,10] The sheet−sheet distance in the protofilament is calculated as the average of the distance between the Cα of residue 12 of peptide i and the closest Cα of residue 36 of another peptide (peptide j) and the distance between the Cα of residue 13 of peptide i and the Cα of residue 35 of peptide j. The radius is defined as the maximum distance among all the Cα atoms of a peptide to the rotational axis of the protofilament.

The quality of the constructed protofilaments was examined using Procheck[14] and through energy minimization using AMBER10.[15] In this calculation, the side chains of a

dx.doi.org/10.1021/ci300300e | J. Chem. Inf. Model. XXXX, XXX, XXX−XXX

protofilament were minimized for 1000 steps and then the whole structure was minimized for 5000 steps.

Definition of Data Sets from Simulations.[12] EPR-constrained simulated annealing molecular dynamics calculations[12] gave protofilament models with helical pitches ranging from 250 to 1000 Å and a stagger of about three peptides. Four data sets (each with 10 models of 101-peptide protofilaments) were obtained from these calculations. Here, we refer to these data sets as 4_nc, 4_250, 4_500, and 4_1000 based on the helical pitch constraint: no constraint (nc), and 250, 500, and 1000 Å, respectively; with four referring to placement of a spin label on every fourth peptide. The details of these calculations have been described elsewhere.[12]

RESULTS

Construction of Protofilament Models with Varied Stagger, Pitch, and Offset. MFIBRIL was used to build idealized protofilament models with variation of stagger, pitch, and offset. Fifty peptides with the highest Cα score were selected from each of the data sets 4_nc, 4_250, 4_500, and 4_1000. Each combination of stagger, pitch, and offset was used to reorient the peptide (Figure 2) and then the side chain direction for each peptide were compared with the consensus directions obtained as indicated in Supporting Information Table S1. Peptides were excluded if they did not meet the following criteria: an exact match for side chains defined as "IN" or "OUT", except for residues 12 and 36; and no more than two differences for side chains defined as "in" and "out". We note that the side chain directions of a given peptide can alter with variation of stagger. A peptide was also excluded if the protofilament built from the peptide had a negative sheet−sheet distance (i.e., a clash between β-sheets).

The results of this procedure for protofilament models no. 1 to no. 15 are shown in Table 1. For example, for model no. 1, there were 18, 19, 24, and 19 peptides from data sets 4_nc, 4_250, 4_500, and 4_1000 (out of the original 50 selected from each data set) that were not excluded by the above criteria. For model no. 1, this gave a total of 80 peptides (Table 1) that were used to build 80 different idealized protofilaments with stagger = 3 peptides, pitch 250 Å, and offset = center (Figure 2). The sheet−sheet distance and radius were determined for each of these protofilaments and are given as an average ± SD in Table 1. A similar procedure was performed for a systematic set of protofilaments with varied stagger, pitch, and offset. Some examples are shown as models no. 2 to no. 15 in Table 1. These results are described in more detail in the following sections.

Model nos. 1 to 15 built from the peptide in Figure 3A were also successfully minimized in AMBER10 (Supporting Information Table S2) and the minimized structures had most residues in allowed regions of conformational space based on Procheck analysis. These results indicate that the models constructed in MFIBRIL have reasonable intermolecular distances and hydrogen bonding.

Structures of Idealized Protofilaments. Geometric analysis of protofilament model nos. 1, 2, and 3 (Table 1) gave sheet−sheet distances of 8.3 ± 1.6, 10.6 ± 1.6, and 11.7 ± 1.7 Å, respectively. These values were similar to those of 8.8 ± 0.3, 10.8 ± 0.2, and 12.6 ± 0.4 Å in the respective simulation data sets 4_250, 4_500, and 4_1000.[12] These results show that MFIBRIL can be used to idealize the simulation model without loss of the key geometric features.

Construction of protofilaments corresponding to model nos. 1, 2, and 3 is shown in Figure 3, based on a single peptide selected from data set 4_500. This peptide (Figure 3A) had the top Cα score among the 1010 peptides (10 models × 101 peptides) in this data set and had side-chain directions that were largely consistent with the consensus directions (Table 1). A discussion of these side-chain directions and a comparison with those in previous structures[11,16] is given later in the text.

Multiple copies of the peptide in Figure 3A were used to construct a protofilament with a stagger of three peptides and a left-handed pitch of 500 Å (Figure 3B). Simplified images of this protofilament and those with pitches of 250 and 1000 Å (built from the same peptide) are shown in Figure 3C. In these images, the peptides are colored blue, orange, and green to illustrate the three-peptide stagger.

Variation of Stagger and Pitch. The general dependence of the sheet−sheet distance on pitch and stagger is shown in Figure 4. A decrease in stagger or an increase in pitch causes an

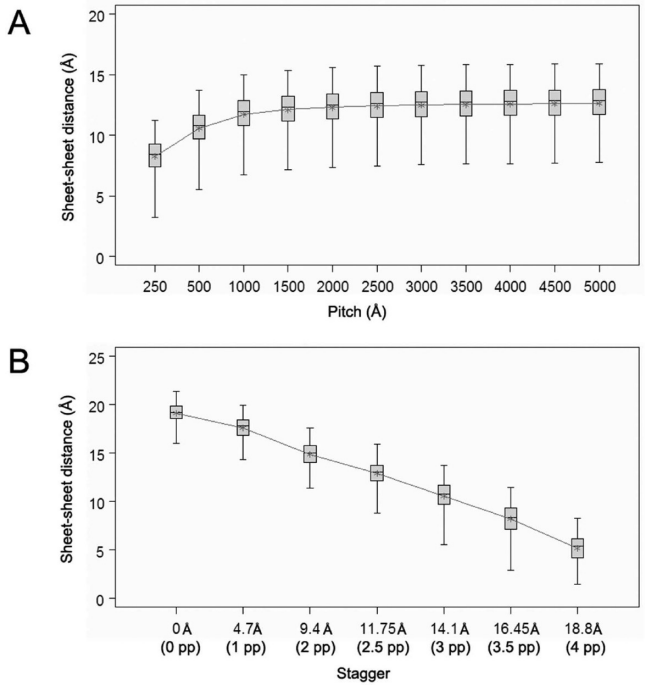

Figure 4. (A) Dependence of the sheet−sheet distance on pitch in a protofilament built in MFIBRIL with a stagger of three peptides. (B) Dependence of the sheet−sheet distance on peptide stagger (shown as the distance with the number of peptides in parentheses) in a protofilament built in MFIBRIL as a left-handed helix with a pitch of 500 Å.

increase in the sheet−sheet distance. At large pitches (>1000 Å), the rate of increase in the sheet−sheet distance is slow, and this distance approaches the value for a straight protofilament with the same stagger. The experimental value for the sheet−sheet distance (about 9.5 Å)[9] is not satisfied for a protofilament with a pitch of 2000 Å and a stagger of three peptides (model no. 4, Table 1) or with a stagger of two or four peptides and a pitch of 500 Å (model nos. 5 and 6 in Table 1). Thus, the experimental sheet−sheet distance is only obtained in protofilaments with pitches of about 250−500 Å (Figure 4A) and a stagger of about three peptides (14.1 Å; Figure 4B).

Variation of Offset. The results in the previous section assume a helical axis that is positioned centrally with respect to

dx.doi.org/10.1021/ci300300e | J. Chem. Inf. Model. XXXX, XXX, XXX−XXX

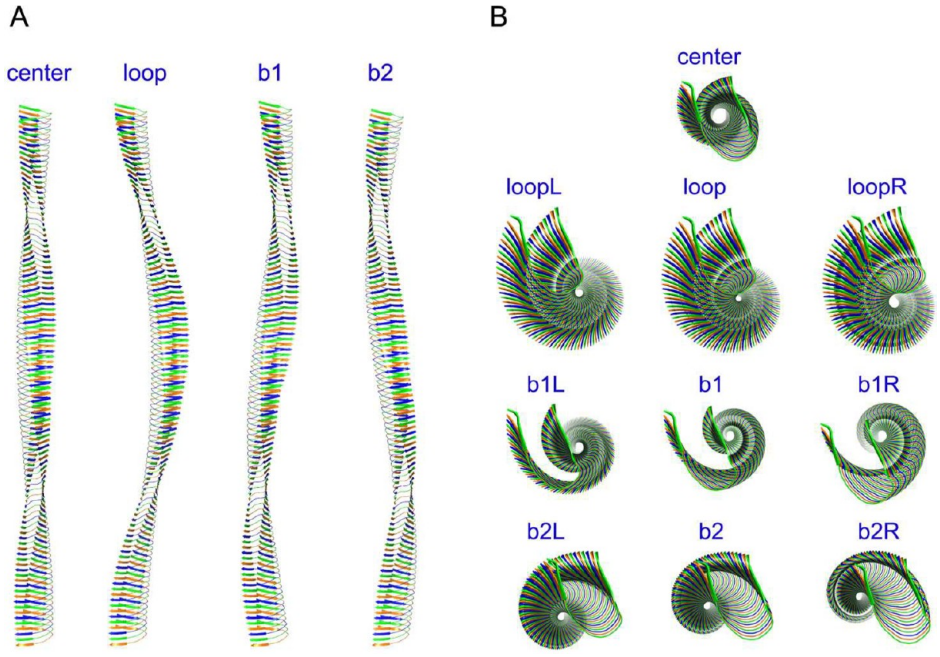

Figure 5. (A) Protofilament models (101 peptides) built in MFIBRIL with a stagger of three peptides and a left-handed helical pitch of 500 Å, using axis offset points indicated in blue (refer to Figure 2D). Successive peptides are colored green, orange, and blue. (B) Protofilament models (three-peptide stagger, 500 Å pitch) viewed along the helical axis, with construction based on the axis offset points shown in Figure 2D.

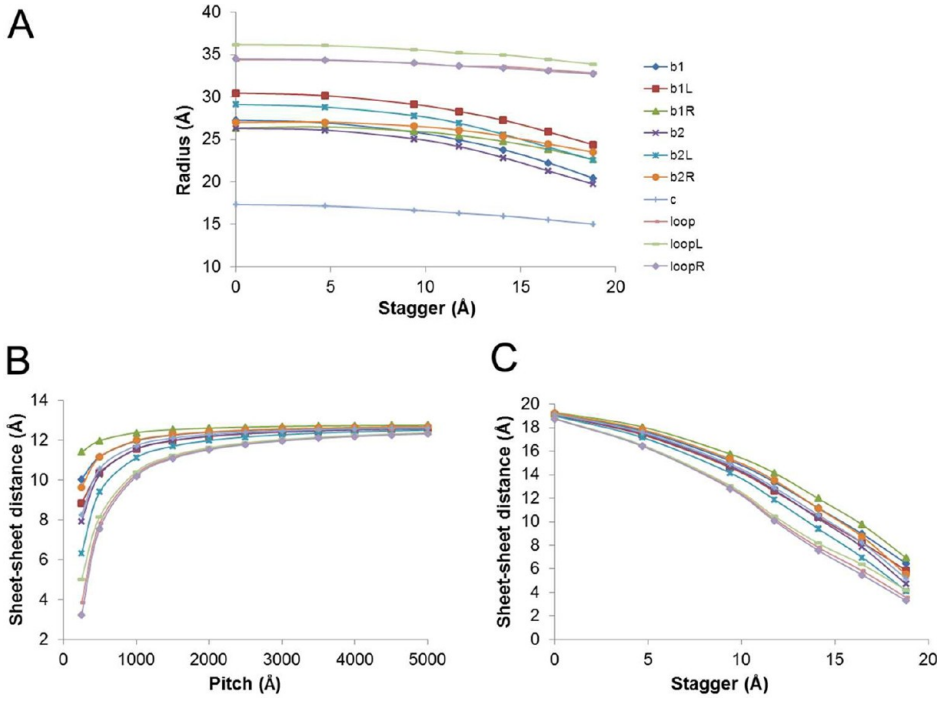

Figure 6. (A) Dependence of the protofilament radius on stagger (shown in ångstrom: 1 peptide stagger = 4.7 Å) in protofilaments built in MFIBRIL with a left-handed helical pitch of 500 Å and using the indicated axis offset points. (B and C) Dependence of the sheet−sheet distance on (B) pitch (with stagger fixed at three peptides) and (C) stagger (with pitch fixed at 500 Å) in protofilaments built using the axis offset points indicated in A.

the hIAPP monomers. However, wrapping of multiple protofilaments around each other to give fibrils is likely to require this axis to be offset from the central position. MFIBRIL models built with inclusion of this offset are shown in Figure 5, and the corresponding geometric data are shown in Table 1 and Figure 6. The structures in Figure 6A all have a pitch of 500 Å and a stagger of three peptides, with offsets (defined in Figure 2) of center, loop, b1, and b2. These structures are examples of those in model nos. 2, 8, 11, and 14, respectively (Table 1). All were built using the peptide in Figure 3A.

The protofilament radius differs significantly with use of different offsets (Figure 6A). Offsets around the loop region give the largest radius (about 35 Å). This feature can be seen in

dx.doi.org/10.1021/ci300300e | J. Chem. Inf. Model. XXXX, XXX, XXX−XXX

the structures in Figure 5B for the loopL, loop, and loopR offsets. The offset of "center" gives the smallest radius (about 17.5 Å), while the β-strand offsets (b1L, b1, b1R, b2L, b2, and b2R) give similar radii of about 23−28 Å with a stagger of 14.1 Å (three peptides). The images in Figure 5B also show how different offsets result in different potential interaction interfaces for protofilament−protofilament interactions. These interfaces would occur close to the offset axis, which appears as the "hole" in the models in Figure 5B.

Different offsets resulted in a smaller variation in sheet−sheet distances (Figure 6B and C). Thus, the conclusion that the experimental sheet−sheet distance is obtained for protofilament pitches of 250 to 500 Å and a stagger of about three peptides (14.1 Å) holds almost regardless of the offset used (Table 1).

DISCUSSION

The MFIBRIL algorithm permits generation of idealized protofilaments based on models from simulation. The idealized models keep the important features of the simulation models but are more ordered. These idealized protofilaments are suitable for further model building of hIAPP fibrils, which can also be achieved in MFIBRIL. Beyond the specific application to hIAPP, MFIBRIL can be used for building any fibrillar aggregate of identical peptides. Polymorphism is common for amyloid proteins, including amyloid β- and α-synuclein, and recent theories suggest that different conformations of amyloid aggregates may play distinct roles in disease.[17] Thus, studying the structural details may reveal different aggregation mechanisms that have different roles in disease. Idealized models generated in MFIBRIL will also provide targets for screening for potential biomarkers and therapeutic agents using docking techniques.

The results obtained with variation of stagger and pitch in MFIBRIL indicate that hIAPP protofilaments may be limited to staggers of about two to four peptides (centered on three) and pitches between about 250 and 500 Å. These parameters gave a sheet−sheet distance and a protofilament radius consistent with experimental data[9,10] and in line with our EPR-constrained simulation models.[12] As stagger approaches four peptides or the pitch decreases to <250 Å, sheet−sheet clashes prevent formation of the protofilament. Conversely, as the stagger falls below two or the pitch increases to 1000 Å and above, the protofilament structure opens up and hydrophobic surfaces within the horseshoe peptide conformation have greater exposure to water. The balance between these extremes may provide the most stable protofilament.

Early models proposed for hIAPP fibrils contained three β-strands in a hIAPP monomer,[18,19] but most recent models have a horseshoe-shaped monomer formed by only two β-strands.[11,12,16] Luca et al.[11] determined a model for ribbonlike hIAPP fibrils using scanning transmission EM, solid state NMR (SSNMR), and modeling,[11] in which each peptide has a horseshoe shape formed by a β-strand (8−16), a connection region (17−27), and a second β-strand (28−37). Molecular dynamics (MD) simulations based on this model indicated potential formation of fibrils containing two or three protofilaments with different organizations and interaction interfaces.[20,21] Further important structural information has been derived by Wiltzius et al.[16] from X-ray structures of several hIAPP fragments, including NFLVHSS (residues 14−20), NNFGAIL (21−27), and SSTNVG (28−33).[16]Hamiltonian-temperature replica exchange MD simulations indicated β-strands for residues 17−26 and 30−35 in a hIAPP dimer.[22] Another study using NMR, atomic force microscopy and mass spectroscopy revealed that IAPP molecules associate into transient low-order oligomers via interactions between H18 and Y37, and simulations based on this finding rendered a two-fold (2-protofilament) model[23] similar to that in the work fo Luca et al.[11] A three-fold model was proposed from two-dimensional infrared spectroscopy and MD simulations.[24]

hIAPP fragments of residues 20−29,[25] 30−37,[26] and 8−20[27] are sufficient to form fibrils in vitro, where 20−29 is the amyloidogenic region, and FLVHS (15−19) and NFLVH (14−18) are the two shortest fragments that have been found to self-assemble.[28] A screening study of hIAPP mutants also revealed the importance of regions 20−29 and 12−17 in fibril formation, with most of the 28 mutations that reduced amyloidogenesis located in these two regions.[29] Residue 20 is important for fibrilization, since an S20G mutation increased in vitro amyloidogenicity and an S20K mutation greatly delayed fibrilization.[30] The aromatic residues in hIAPP also play an important role in fibrilization. Substituting one or all the aromatic residues with Leu and Ala decreased the rate of fibril formation,[31,32] and fluorescence resonance energy transfer has shown that Y37 interacts with at least one Phe residues during fibrillization.[33] It has recently been shown that the effects of the aromatic side chains in fibril formation are likely to be due to their hydrophobicity and planarity.[34] The nonamyloidogenic rat IAPP differs from hIAPP at only six residues at positions 18, 23, 25, 26, 28, and 29, including three key proline residues (P25, P28, P29) that play a major role in preventing fibril formation.[35]

Since previous studies have identified residues 20−29 as the key amyloidogenic region, it is of interest to evaluate the consistency of side chain orientations in this region among the proposed models. In Table 2, we compare the side chain orientations of the "consensus" peptide derived in this work

Table 2. Side-Chain Directions in the Loop Region of hIAPP in Protofilaments

amino acid	consensus[a]	representative peptide[b]	Luca et al.[11,c]	Wiltzius et al.[16,d]
S20	out	OUT	O	
N21	i/o	OUT	O	→
N22	i/o	OUT	I	←
*F*23	out	OUT	O	→
G24	out	OUT	−	
A25	in	IN	I	→
I26	out	OUT	O	←
L27	i/o	IN	I	→
S28	out	OUT	O	
S29	in	IN	I	
T30	OUT	OUT	O	

[a]Consensus side chain directions from simulations constrained by EPR data.[12] "OUT" and "out" indicate >80% and >60% of side chains pointing to the outside of the protofilament, respectively; "IN" (see Supporting Information Table S1) and "in" indicate >80% and >60% of side chains are pointing inward, respectively; "i/o" indicates none of these criteria were met. Data are taken from simulations described in ref 12. [b]A representative peptide (Figure 3A) determined in this work (also see Supporting Information Table S1). [c]Taken from Figure 11 of ref 11, O and I indicate side chains pointing to the outside and inside of the peptide hairpin, respectively. "−" indicates that the direction could not be determined from the figure. [d]Data from the X-ray structure[16] for peptide NNFGAIL (21−27) (PDB ID 3DGJ), with relative side chain directions shown for two halves of the peptide.

dx.doi.org/10.1021/ci300300e | J. Chem. Inf. Model. XXXX, XXX, XXX−XXX

with those in two other models.[11,16] There is excellent agreement between the side chain orientations in this region in our consensus peptide and those in Luca et al.[11] Interestingly, we also observe good agreement with the X-ray structure of NNFGAIL (21−27),[16] based on viewing this peptide as two halves separated by a flexible glycine residue. On this basis, the alternating inward and outward patterns observed in Luca et al.[11] and in our consensus peptide (with the exception of N22, which we cannot define) are also seen in the NNFGAIL X-ray structure.[16] The general consistency among the models provides a good basis for further use of these orientations in theoretical studies.

The SSNMR of the Luca et al.[11] model suggests a structure comprising two protofilaments that interact with each other through the C-terminal β-sheet. Consistent with this interaction, the X-ray structure of peptide SSTNVG (28−33)[16] has a steric zipper interface between two peptides, which may also be present in the hIAPP fibril. Recent studies using ion mobility spectrometry combined with mass spectrometry and molecular simulation have also suggested that the interfaces of hIAPP dimers are formed by β-strands.[36] However, the orientation of the side chains of the beta strands in these models remains uncertain, with several different proposed models.[11,12,16]

Putative models for fibrils based on the structural and mutagenesis information described above can be tested through construction of idealized structures in MFIBRIL. Indeed, our main goal in developing the program is to build experimentally testable models for amyloid fibrils with defined staggers, pitches, and offsets. The initial definition of the layer will be based on the proposed peptide−peptide interactions in a particular fibril, with two or more interacting protofilaments. It is likely that only specific combinations of stagger, pitch, and offset will be viable for a particular assembly, based on steric considerations only, and this will limit the number of models. For models that are sterically viable, we can then determine pairwise interspin label distances for multiple pairs of sites using another algorithm in our laboratory, PRONOX.[37] With this algorithm, we can generate data in a form consistent with that obtained from EPR DEER experiments, which may allow the predicted data to be validated experimentally.

■ ASSOCIATED CONTENT

Supporting Information

More information on side chain orientations and energy minimization This material is available free of charge via the Internet at http://pubs.acs.org.

■ AUTHOR INFORMATION

Corresponding Author

*Tel.: 323 442-3310. Fax: 323 442-1369. E-mail: ihaworth@usc.edu.

Notes

The authors declare no competing financial interest.

■ ACKNOWLEDGMENTS

Computation for the work described in this paper was supported by the University of Southern California Center for High-Performance Computing and Communications (www.usc.edu/hpcc). Funding was provided by the NIH (AG027936) to R.L.

■ REFERENCES

(1) Margittai, M.; Langen, R. Fibrils with parallel in-register structure constitute a major class of amyloid fibrils: molecular insights from electron paramagnetic resonance spectroscopy. *Q. Rev. Biophys.* **2008**, *41*, 265−297.

(2) Woods, S. C.; Lutz, T. A.; Geary, N.; Langhans, W. Pancreatic signals controlling food intake; insulin, glucagon and amylin. *Philos. Trans. R. Soc. Lond. B Biol. Sci.* **2006**, *361*, 1219−1235.

(3) Meier, J. J.; Kayed, R.; Lin, C. Y.; Gurlo, T.; Haataja, L.; Jayasinghe, S.; Langen, R.; Glabe, C. G.; Butler, P. C. Inhibition of human IAPP fibril formation does not prevent beta-cell death: evidence for distinct actions of oligomers and fibrils of human IAPP. *Am. J. Physiol. Endocrinol. Metab.* **2006**, *291*, E1317−E1324.

(4) Zraika, S.; Hull, R. L.; Verchere, C. B.; Clark, A.; Potter, K. J.; Fraser, P. E.; Raleigh, D. P.; Kahn, S. E. Toxic oligomers and islet beta cell death: guilty by association or convicted by circumstantial evidence? *Diabetologia* **2010**, *53*, 1046−1056.

(5) Chiti, F.; Dobson, C. M. Protein misfolding, functional amyloid, and human disease. *Annu. Rev. Biochem.* **2006**, *75*, 333−366.

(6) Jayasinghe, S. A.; Langen, R. Identifying structural features of fibrillar islet amyloid polypeptide using site-directed spin labeling. *J. Biol. Chem.* **2004**, *279*, 48420−48425.

(7) Higham, C. E.; Jaikaran, E. T.; Fraser, P. E.; Gross, M.; Clark, A. Preparation of synthetic human islet amyloid polypeptide (IAPP) in a stable conformation to enable study of conversion to amyloid-like fibrils. *FEBS Lett.* **2000**, *470*, 55−60.

(8) Kayed, R.; Bernhagen, J.; Greenfield, N.; Sweimeh, K.; Brunner, H.; Voelter, W.; Kapurniotu, A. Conformational transitions of islet amyloid polypeptide (IAPP) in amyloid formation in vitro. *J. Mol. Biol.* **1999**, *287*, 781−796.

(9) Sumner Makin, O.; Serpell, L. C. Structural characterisation of islet amyloid polypeptide fibrils. *J. Mol. Biol.* **2004**, *335*, 1279−1288.

(10) Goldsbury, C. S.; Cooper, G. J.; Goldie, K. N.; Muller, S. A.; Saafi, E. L.; Gruijters, W. T.; Misur, M. P.; Engel, A.; Aebi, U.; Kistler, J. Polymorphic fibrillar assembly of human amylin. *J. Struct. Biol.* **1997**, *119*, 17−27.

(11) Luca, S.; Yau, W. M.; Leapman, R.; Tycko, R. Peptide conformation and supramolecular organization in amylin fibrils: constraints from solid-state NMR. *Biochemistry* **2007**, *46*, 13505−13522.

(12) Bedrood, S.; Li, Y.; Isas, J. M.; Hegde, B. G.; Baxa, U.; Haworth, I. S.; Langen, R. Fibril structure of human islet amyloid polypeptide. *J. Biol. Chem.* **2012**, *287*, 5235−5241.

(13) *The PyMOL Molecular Graphics System*, version 1.3r1; Schrödinger, LLC, 2010.

(14) Laskowski, R. A.; MacArthur, M. W.; Moss, D. S.; Thornton, J. M. PROCHECK: a program to check the stereochemical quality of protein structures. *J. App. Cryst.* **1993**, *26*, 283−291.

(15) Case, D. A.; Cheatham, T. E., 3rd; Darden, T.; Gohlke, H.; Luo, R.; Merz, K. M., Jr.; Onufriev, A.; Simmerling, C.; Wang, B.; Woods, R. J. The AMBER biomolecular simulation programs. *J. Comput. Chem.* **2005**, *26*, 1668−1688.

(16) Wiltzius, J. J.; Sievers, S. A.; Sawaya, M. R.; Cascio, D.; Popov, D.; Riekel, C.; Eisenberg, D. Atomic structure of the cross-beta spine of islet amyloid polypeptide (amylin). *Protein Sci.* **2008**, *17*, 1467−1474.

(17) Reinke, A. A.; Gestwicki, J. E. Insight into amyloid structure using chemical probes. *Chem. Biol. Drug Des.* **2011**, *77*, 399−411.

(18) Jaikaran, E. T.; Clark, A. Islet amyloid and type 2 diabetes: from molecular misfolding to islet pathophysiology. *Biochim. Biophys. Acta* **2001**, *1537*, 179−203.

(19) Kajava, A. V.; Aebi, U.; Steven, A. C. The parallel superpleated beta-structure as a model for amyloid fibrils of human amylin. *J. Mol. Biol.* **2005**, *348*, 247−252.

(20) Zhao, J.; Yu, X.; Liang, G.; Zheng, J. Structural polymorphism of human islet amyloid polypeptide (hIAPP) oligomers highlights the importance of interfacial residue interactions. *Biomacromolecules* **2011**, *12*, 210−220.

(21) Zhao, J.; Yu, X.; Liang, G.; Zheng, J. Heterogeneous triangular structures of human islet amyloid polypeptide (amylin) with internal hydrophobic cavity and external wrapping morphology reveal the polymorphic nature of amyloid fibrils. *Biomacromolecules* **2011**, *12*, 1781−1794.
(22) Laghaei, R.; Mousseau, N.; Wei, G. Structure and thermodynamics of amylin dimer studied by Hamiltonian-temperature replica exchange molecular dynamics simulations. *J. Phys. Chem. B* **2011**, *115*, 3146−3154.
(23) Wei, L.; Jiang, P.; Xu, W.; Li, H.; Zhang, H.; Yan, L.; Chan-Park, M. B.; Liu, X. W.; Tang, K.; Mu, Y.; Pervushin, K. The molecular basis of distinct aggregation pathways of islet amyloid polypeptide. *J. Biol. Chem.* **2011**, *286*, 6291−6300.
(24) Wang, L.; Middleton, C. T.; Singh, S.; Reddy, A. S.; Woys, A. M.; Strasfeld, D. B.; Marek, P.; Raleigh, D. P.; de Pablo, J. J.; Zanni, M. T.; Skinner, J. L. 2DIR spectroscopy of human amylin fibrils reflects stable beta-sheet structure. *J. Am. Chem. Soc.* **2011**, *133*, 16062−16071.
(25) Westermark, P.; Engstrom, U.; Johnson, K. H.; Westermark, G. T.; Betsholtz, C. Islet amyloid polypeptide: pinpointing amino acid residues linked to amyloid fibril formation. *Proc. Natl. Acad. Sci. U.S.A.* **1990**, *87*, 5036−5040.
(26) Nilsson, M. R.; Raleigh, D. P. Analysis of amylin cleavage products provides new insights into the amyloidogenic region of human amylin. *J. Mol. Biol.* **1999**, *294*, 1375−1385.
(27) Jaikaran, E. T.; Higham, C. E.; Serpell, L. C.; Zurdo, J.; Gross, M.; Clark, A.; Fraser, P. E. Identification of a novel human islet amyloid polypeptide beta-sheet domain and factors influencing fibrillogenesis. *J. Mol. Biol.* **2001**, *308*, 515−525.
(28) Mazor, Y.; Gilead, S.; Benhar, I.; Gazit, E. Identification and characterization of a novel molecular-recognition and self-assembly domain within the islet amyloid polypeptide. *J. Mol. Biol.* **2002**, *322*, 1013−1024.
(29) Fox, A.; Snollaerts, T.; Errecart Casanova, C.; Calciano, A.; Nogaj, L. A.; Moffet, D. A. Selection for nonamyloidogenic mutants of islet amyloid polypeptide (IAPP) identifies an extended region for amyloidogenicity. *Biochemistry* **2010**, *49*, 7783−7789.
(30) Cao, P.; Tu, L. H.; Abedini, A.; Levsh, O.; Akter, R.; Patsalo, V.; Schmidt, A. M.; Raleigh, D. P. Sensitivity of amyloid formation by human islet amyloid polypeptide to mutations at residue 20. *J. Mol. Biol.* **2012**, *421*, 282−295.
(31) Marek, P.; Abedini, A.; Song, B.; Kanungo, M.; Johnson, M. E.; Gupta, R.; Zaman, W.; Wong, S. S.; Raleigh, D. P. Aromatic interactions are not required for amyloid fibril formation by islet amyloid polypeptide but do influence the rate of fibril formation and fibril morphology. *Biochemistry* **2007**, *46*, 3255−3261.
(32) Tracz, S. M.; Abedini, A.; Driscoll, M.; Raleigh, D. P. Role of aromatic interactions in amyloid formation by peptides derived from human Amylin. *Biochemistry* **2004**, *43*, 15901−15908.
(33) Padrick, S. B.; Miranker, A. D. Islet amyloid polypeptide: identification of long-range contacts and local order on the fibrillogenesis pathway. *J. Mol. Biol.* **2001**, *308*, 783−794.
(34) Doran, T. M.; Kamens, A. J.; Byrnes, N. K.; Nilsson, B. L. Role of amino acid hydrophobicity, aromaticity, and molecular volume on IAPP(20−29) amyloid self-assembly. *Proteins* **2012**, *80*, 1053−1065.
(35) Green, J.; Goldsbury, C.; Mini, T.; Sunderji, S.; Frey, P.; Kistler, J.; Cooper, G.; Aebi, U. Full-length rat amylin forms fibrils following substitution of single residues from human amylin. *J. Mol. Biol.* **2003**, *326*, 1147−1156.
(36) Dupuis, N. F.; Wu, C.; Shea, J. E.; Bowers, M. T. The amyloid formation mechanism in human IAPP: Dimers have beta-strand monomer-monomer interfaces. *J. Am. Chem. Soc.* **2011**, *133*, 7240−7243.
(37) Hatmal, M. M.; Li, Y.; Hegde, B. G.; Hegde, P. B.; Jao, C. C.; Langen, R.; Haworth, I. S. Computer modeling of nitroxide spin labels on proteins. *Biopolymers* **2012**, *97*, 35−44.